Molecular Crystals and Liquid Crystals
Publication details, including instructions for authors and subscription information:
http://www.tandfonline.com/loi/gmcl20

Talbot Effect from Rotational Symmetry Gratings: Application to 3D Refractive Grating Formation

A. Badalyan [a], R. Hovsepyan [a], V. Mekhitaryan [a], P. Mantashyan [a] & R. Drampyan [a]

[a] Institute for Physical Research, National Academy of Sciences of Armenia

Version of record first published: 13 Jun 2012.

To cite this article: A. Badalyan , R. Hovsepyan , V. Mekhitaryan , P. Mantashyan & R. Drampyan (2012): Talbot Effect from Rotational Symmetry Gratings: Application to 3D Refractive Grating Formation, Molecular Crystals and Liquid Crystals, 561:1, 57-67

To link to this article: http://dx.doi.org/10.1080/15421406.2012.686711

Mol. Cryst. Liq. Cryst., Vol. 561: pp. 57–67, 2012

ISSN: 1542-1406 print/1563-5287 online
DOI: 10.1080/15421406.2012.686711

Taylor & Francis
Taylor & Francis Group

Talbot Effect from Rotational Symmetry Gratings: Application to 3D Refractive Grating Formation

A. BADALYAN, R. HOVSEPYAN, V. MEKHITARYAN, P. MANTASHYAN, AND R. DRAMPYAN*

Institute for Physical Research, National Academy of Sciences of Armenia

We report the first observation of Talbot effect – diffraction grating images self-replications at regular distances, from 1D annular grating with the period of $d = 30 \pm 1$ μm. Up to 20 high contrast revivals of the grating were observed by the green laser beam at $\lambda = 532$ nm with Talbot distance $Z_T = d^2/\lambda = 1.57 \pm 0.01$ mm. The grating self imaging with half period of the original grating at $Z_T/2$ was also observed. Using the annular grating as a mask, the recording of refractive index photonic lattice in 2 mm thick Fe doped lithium niobate crystal was performed by 532 nm laser beam. The replication of the grating images due to Talbot effect provides the recording of two refractive replicas of the grating with the periods of d and d/2 inside the 2 mm crystal checked by phase microscope depth scan observations. The obtained results show the possibility of the use of 2D masks for the creation of 3D photonic lattices in photorefractive materials, which can be used as photonic crystals.

Keywords diffraction gratings; laser; photonic lattice; Talbot effect

1. Introduction

Optical patterns formation with desired intensity distribution has received a great deal of attention concerning the fabrication of micro- and nanometric scale photonic lattices, where 1,2 and 3-dimensional (1D, 2D and 3D) intensity distributions are recorded in photosensitive materials [1–3], such as photorefractive crystals [4], liquid crystals [5,6] and composite polymer materials, including polymer dispersed [7] and polymer stabilized liquid crystals [8–10], photopolymerizable zol-gel glass [11] and its modifications [12–14], as well as in atomic vapors [15,16]. In spite of these methods provide relatively low refractive index modulation, compared with the techniques of fabrication of artificial periodic structures by lithography, electronic beam or etching in high refractive index materials (photonic crystals [17–20]), nevertheless such photonic lattices are very promising for the information storage and readout [21], for controlling and manipulating the flow of light [4,20], for the formation of two-dimensional spatial solitons [22]. The computer generated holographic technique [2] and recently suggested Bessel beam method [23] and combined interferometric–mask technique [24] are very promising for the creation of 2D and 3D spatial periodic structures in photorefractive materials. 2D photonic lattices are promising as guiding and trapping systems and for different optical devices. However, the higher 3D volume photonic lattices

*Address correspondence to Institute for Physical Research, National Academy of Sciences of Armenia, 0203, Ashtarak, Armenia. Tel: (374 10) 288150; Fax: (374 232) 3 11 72. E-mail: rdramp@ipr.sci.am; paytsar.mantashyan@gmail.com

are of a great interest for high capacity optical storage, optical computers, optical communication etc. Thus, in spite of many successes in this field, the elaboration and realization of new methods for optical formation of 2D and 3D lattices is an actual problem. One of the ways to create 3D photonic lattices is the application of Talbot effect – self-imaging phenomenon [25] to the lattices formation.

The Talbot effect is a near field diffraction effect the essence of which is the self replication of the diffraction grating image away from the grating at regular distances (Talbot length), equaled to $Z_T = d^2/\lambda$, where d is the period of the grating and λ is the wavelength of the light incident on the grating [25]. One of the interesting features of Talbot effect is the fractional revivals of the gratings, when at fractional Talbot distances sub-images with smaller grating periods can also be observed. In spite of the Talbot effect was discovered over than 150 years ago for one dimensional rule diffraction gratings [26] and explained by Lord Rayleigh as a near field diffraction effect [27], now it is finding the renewed interest for formation of volume photonic lattices. The complete theory of Talbot effect is given in [28] and various applications of Talbot effect both for photonics and atom optics were discussed and realized in different works (see, for example, [15,25,29–38] and references therein).

Obviously, Talbot effect is very promising for the creation of 2D and 3D photonic lattices with the use of lower dimensional 1D and 2D transverse gratings, due to Talbot self-replication effect in the axial direction. Moreover, the exciting feature of Talbot effect to produce smaller fractional revivals of the gratings opens new possibilities for potential applications. Particularly, at half Talbot distance the replication of the grating image with half of original grating period takes place. This opens a way for construction of nano-scale photonic lattices with the use of micrometric scale gratings. Of course, there are limits to how small these structures can get. Particularly, the contrast of revivals decreases with the size of fractional period.

In this paper we report the technique of optical induction of 2D and 3D periodic lattices in photorefractive materials based on rotational symmetry diffraction grating Talbot self-replications. 1D and 2D different rotational symmery diffraction masks with the periods of few tens micrometers were prepared. The 532 nm cw laser beam was used in experiments to form an intensity modulated light beam profile and recording of photonic lattices in Fe doped lithium niobate crystals (LN:Fe). The spatial modulated intensity pattern from 1D annular mask with 100 circles and $\sim$30 μm radial period was imparted into the phororefractive LN:Fe crystal via electro-optic effect, thus creating refractive index lattice. The recorded lattice was tested by phase microscope. The observations of depth scan phase microscope images showed the spatial frequency doubling of the recorded lattice due to fractional Talbot effect. The use of 2D different-fold rotational symmetry masks providing light intensity modulation both in radial and azimuthal directions is discussed in the aspect of creation of 3D photonic lattices in photosensitive materials.

2. Observation of Talbot Effect from Annular Mask

2.1. Preparation of Rotational Symmetry Masks and Interferometric Testing

From 1 to 10-fold axial symmetry masks were generated by computer graphic technique developed in [24]. The masks consisted of transparent holes periodically disposed along the equidistantly positioned concentric circles, surrounding the central hole. The number of holes on the i th circle was equaled $M_i = ji$, where $i = 1,2,3\ldots$ is integer and j is the

symmetry order of the mask. The masks of reduced size (0.6 cm) with $i = 100$ were printed by high resolution printer (3300 dpi) on the transparent film. Both the positive and negative masks were prepared. The prepared negative masks had 10–60 μm distances between 10 μm transparent holes located on the opaque disk. The whole mask consisted of ∼35000 holes disposed along the 100 hypothetical concentric circles.

Figure 1 (a–c) show the examples of the fragments of 2, 6–fold and the infinite symmetry negative masks used in the present experiment. Figure 1b shows nearly equidistant

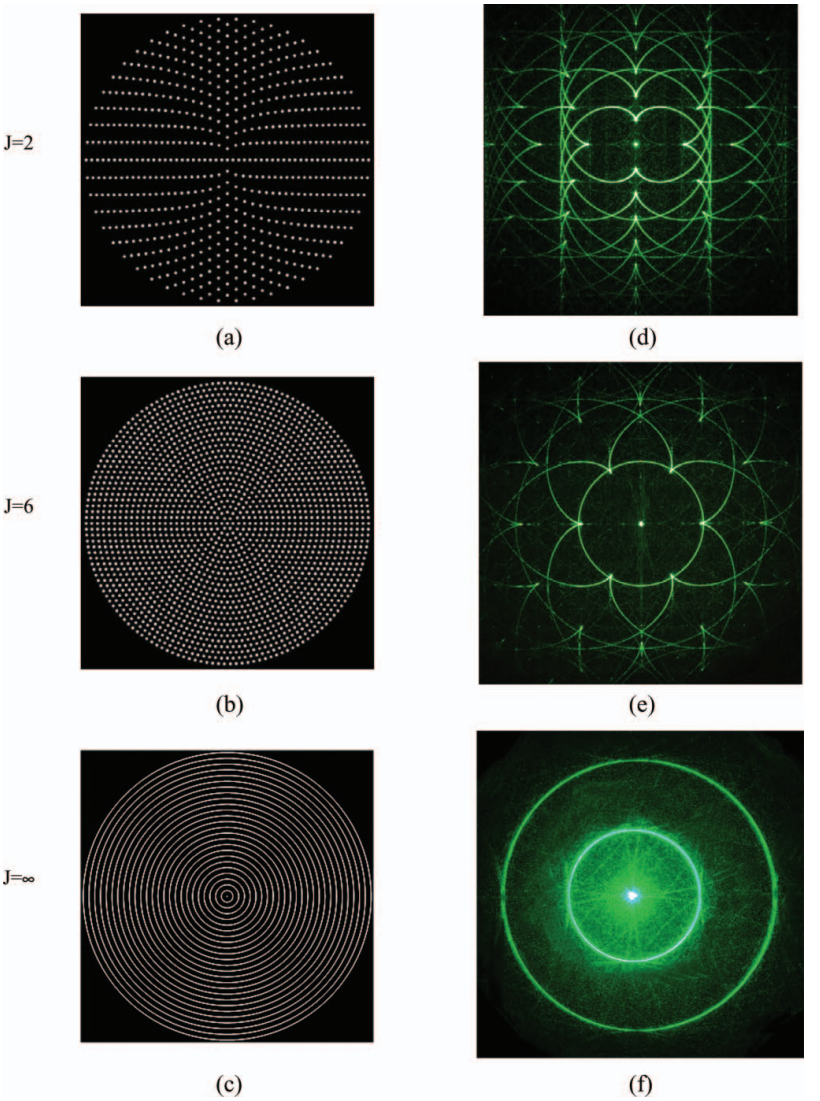

Figure 1. (Color online). Fragments of enlarged patterns of negative 2- and 6-fold and infinite symmetry masks (a–c). The 2- and 6-fold symmetry masks had a diameter of 0.6 cm and a distance around 10–60 μm between ∼10 μm holes. The annular mask had a distance of 30 μm between circles. Corresponding diffraction patterns (d–f) obtained in the far field from the negative 2 and 6-fold symmetry and annular masks (a–c) by green 532 nm laser beam.

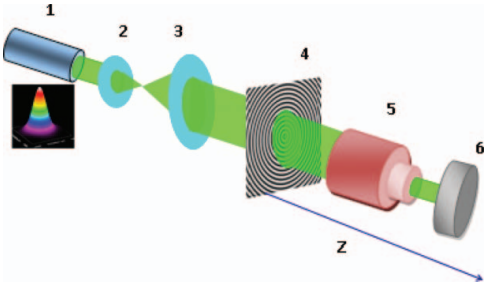

Figure 2. (Color online). Experimental set-up. 1 - laser operating at 532 nm wavelength with radiation power 100 mW. 2, 3 - confocal lenses, 4 - mask, 5 - microscope, 6 - CCD camera. The inset shows the Gaussian intensity distribution of 532 nm laser beam.

disposition of holes in radial and azimuthal directions for 6-fold symmetry mask. The annular mask is two dimensional as a pattern, but one-dimensional as a grating with the period of $\sim$30 μm between circles. The masks were tested by observing the diffraction patterns from the masks in the far field by 532 nm green laser beam. The obtained high contrast diffraction patterns (Fig. 1, d–f) confirm the high quality of the prepared masks.

2.2. Experimental Setup for Observation of Talbot Effect from Annular Mask and Results

Experimental arrangement for the observation of Talbot replications of the rotational symmetry masks and measurement of Talbot distances is shown in Fig. 2. The laser source was single-mode second harmonic of cw YAG:Nd laser at 532 nm wavelength with linear polarization, 100 mW power and 0.7 mm beam diameter. The Gaussian intensity distribution of green 532 nm beam is shown in the inset of Fig. 2. The laser beam was expanded by confocal lenses and illuminated the mask. The mask plane was imaged on the CCD camera by microscope objective. The mask was placed on the table with possibility of micrometric scale moving along the Z axis. As the mask was moved out of the focal plane, the mask image reappeared at Talbot distances. The micrometric moving of the mask allowed the measuring the Talbot distances with high accuracy of 5 μm.

Figure 3 (a–c) show the images of negative annular mask with the period of $d = 30 \pm 1$ μm at $Z = 0$, $Z_T/2$, as well as 20th self-replication, respectively. The measured Talbot distance is equaled to $Z_T = 1.57 \pm 0.01$ mm. The 20th self replication still shows high

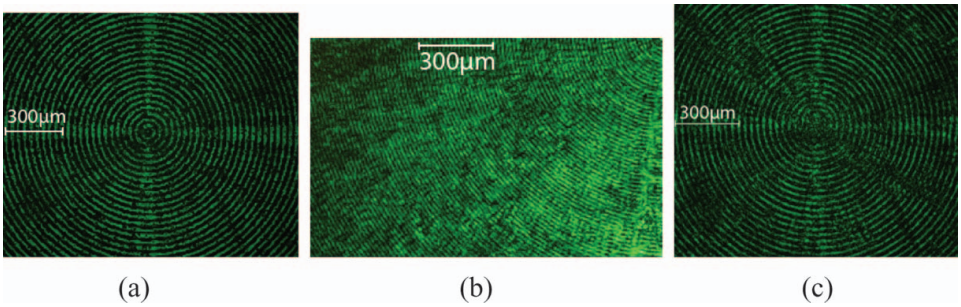

Figure 3. (Color online). Self replications of circular mask at different Talbot distances: (a) $Z_T = 0$, (b) $Z_T/2 = 0.78 \pm 0.01$ mm and (c) $20Z_T = 31.40 \pm 0.01$ mm.

contrast of replicated mask image. Figure 3b shows the spatial frequency 1/*d* doubling of the recorded lattice due to fractional Talbot effect recorded at the distance $Z_T/2 = 0.78 \pm 0.01$ mm.

3. Recording of Photonic Lattice in Photorefractive Fe Doped Lithium Niobate Crystal

3.1. Experimental Setup

The recording of photonic lattice based on Talbot effect is performed in lithium niobate crystals doped with 0,05 wt% Fe taking into account their large photorefractive properties and possibility of creating the long-live photonic lattices for applications. The experimental arrangement for recording of photonic lattice is shown in Fig. 4. The single-mode laser beam at 532 nm wavelength with linear polarization, 100 mW power and 0.7 mm beam diameter was expanded by confocal lenses and after passing through the mask illuminated the crystal. The mask was in touch with the crystal. The optical C-axis of the crystal was oriented along the crystal surface and the polarization of laser beam was directed along the C-axis of the crystal. LN crystal had the dimensions 15 mm × 10 mm × 1.5 mm. The annular mask was used for the recording of photonic lattices in LN:Fe crystal and demonstration of the Talbot replication and frequency doubling of the recorded lattice. The duration of recording was 60 minutes.

3.2. Testing of Recorded Photonic Lattices by Phase Microscope

The photonic lattices recorded in LN:Fe crystal were tested by phase microscope. Figure 5 shows the phase microscope depth scan images of the recorded photonic lattice. The replicated image of the circular lattice near the exit surface of the 2 mm thick crystal is shown in Fig. 5a. The spatial frequency doubling of the recorded lattice due to the fractional Talbot effect was detected by scanning the observation plane to $Z_T/2 = d^2/2\ (\lambda/n_e)$ ($n_e = 2.21$ is extraordinary index of refraction for LN:Fe) toward the input face of the crystal (Fig. 5b).

The used microscope (Union Versamet-2) did not allow the high accuracy measurement of crystal displacement during depth scan. However, such measurements will allow the

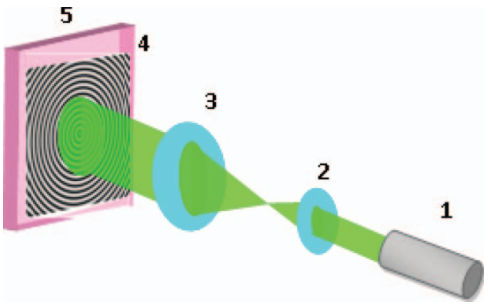

Figure 4. (Color online). Experimental setup for photonic lattices recording in LN:Fe crystal. 1 - laser operating at 532 nm wavelength with radiation power 100 mW. 2, 3 - confocal lenses, 4 - mask, 5 - crystal.

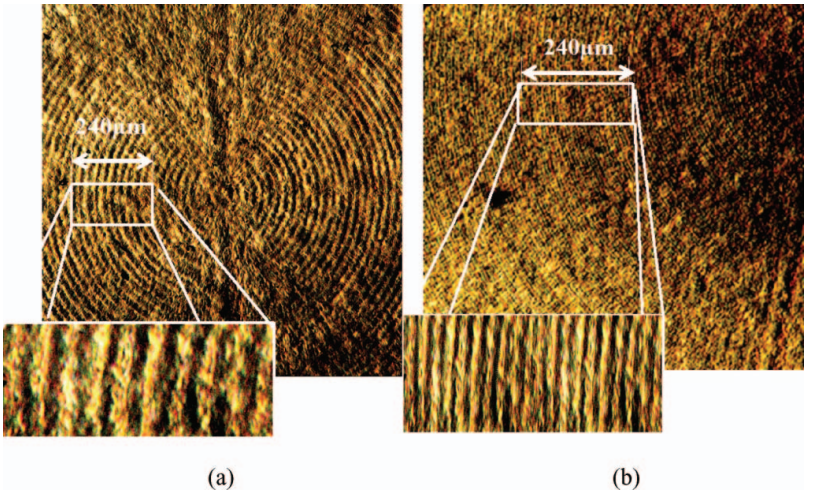

Figure 5. (Color online). Phase microscope depth scan images of photonic lattices recorded inside the LN:Fe crystal by annular mask. (a) replicated image at the exit suface of the crystal. (b) the frequency doubled image of annular mask at $Z_T/2$ toward the input face of the crystal. Insets are enlarged patterns of regions marked by solid white rectangles.

measuring of refractive index of the medium by comparison of high accuracy measurements of Talbot distance of mask replications in the air space and in the medium.

3.3. Physical Mechanism of Recording of Photonic Lattice in LN:Fe Crystal

The physical mechanism of the formation of photonic lattices in photorefractive LN: Fe crystal is based on the electro-optic effect [39–42]. Fe ions occur in LN crystal in different valence states: Fe^{2+} and Fe^{3+}. The green light excites the electrons from Fe^{2+} to the conduction band. The corresponding band diagram is shown in Fig. 6. Electrons migrate in the conduction band and finally are trapped by Fe^{3+}.

The redistribution of the charges builds up an internal electric field E and so changes the refractive index $\Delta n_i = r_{ij}E_j$, where r_{ij} is the electro-optic coefficient. Thus, the inhomogeneous illumination of photorefractive materials leads to the modulation of refractive index. Two main mechanisms – photovoltaic effect and diffusion of photo-induced carriers are responsible for the formation of refractive lattices in photorefractive crystal [39–42].

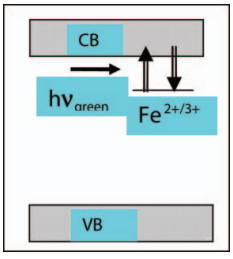

Figure 6. Band diagram of lithium niobate doped with iron. CB is the conduction band, VB is the valence band.

The diffusion effect can be neglected for lattice spatial frequencies less than 10^5 lines /cm [41] which is in case of the present experiment. The electric field induced by photovoltaic effect is due to the charge separation taking place along the C-axis of the crystal [40,41]. Induced electric field is determined by $E_{\mathrm{PV}} = \alpha\, k\, I/\sigma$, where α is the absorption coefficient, k is the Glass constant depending on the nature of absorbing centers and light wavelength, I is the light intensity, σ is conductivity of the illuminated part of the crystal [41,42]. In Fe doped LN crystal the change of extraordinary refractive index is larger than the change of ordinary index by a factor of four [40] and the induced refractive index change Δn is mainly due to the distortion of the extraordinary index of refraction n_{e}.

The life-time of recorded lattices in the doped lithium niobate crystals in the absence of external affects, such as light (dark storage time) and heating is up to one year [43,44]. In particular, the detailed study of the recorded photonic lattices in iron doped lithium niobate crystals showed [45] that the dark storage time varies between few minutes to one year depending on the concentration of the iron and crystal temperature. At room temperature the dark storage time of recorded lattices in 0.05wt% Fe doped lithium niobate crystals used in the present experiment is around one year.

One of the important problems in the practical applications is the erasure of the stored lattices (i.e. stored information) during the read-out by homogeneous light, which results in light diffraction and reconstructs the information encoded in the recording spatially modulated beam. Several techniques including thermal and electrical "fixing" of holograms were developed to overcome this problem [46–48]. But the real-time and all-optical processing and the rapid optical refreshment of memory will give wider possibilities for applications. The required materials should have maximal sensitivity to light in order to increase the recording efficiency and at the same time they should not be affected by illuminating light during readout. One of the ways to avoid the erasure of stored lattice is the read-out by longer wavelength laser beam than the recording wavelength, which prevents the excitation of impurity ion electrons to the conduction band [21]. For many applications it is more convenient to perform the read-out by uniform probe beam at the recording wavelength. Very promising is two-photon recording [49] in materials in which two-photons are required for generation of free electrons. Typically, different wavelengths are chosen for the first and second excitations. Low energy photons contain the holographic information, whereas the high energy photons sensitized the material for recording. During read-out only light at the recording wavelength is used, and nondestructive read-out is achieved. The other method is two-center holographic recording in doubly doped photorefractive crystals, suggested and realized with the use of LN:Fe:Mn crystal and two-beam interference technique in [21]. The doubly doped LN crystals exhibiting photochromic effect provides the high stability of the stored grating during the read-out by weak probe beam at the recording wavelength. The detailed studies of two center recording by Bessel standing wave technique [23] with 17 mW, 532 nm beam in LN crystal doped with 0,05 w% of Fe and Cu showed the persistence of recorded gratings against erasure during 8000 sec when illuminating by 2 mW homogeneous probe beam [50].

4. Prospects for Recording of 3D Photonic Lattices by Rotational Symmetry Masks

The annular mask is two-dimensional as a pattern, but one-dimensional as a grating with the radial period of 30 μm between circles. Thus the Talbot multiple replication of mask image along the axial direction will lead to the formation of 2D photonic lattices in photorefractive medium. The formed photonic lattice is a combination of annular and planar gratings.

The use of different rotational symmetry 2D masks [24] (examples of which are shown in Fig. 1a,b) allowing the spatial modulation of incident light both in radial and azimuthal directions will allow to construct 3D photonic lattices due to additional Talbot self-replications of mask image in the axial direction. The Talbot distance can be easily controlled by periods of mask and light wavelength. The fractional self-replication opens a way for construction of 3D photonic lattices with nano-scale periods using micrometric scale gratings. Of course, the contrast of replicated images decreases with the increase of number of replications. This is the subject of special investigations. Nevertheless, the observation in the present experiment of 20 high contrast replications of annular mask shows that the suggested approach is realistic. The suggested technique for the formation 3D lattices is applicable to any photosensitive or nonlinear materials such as solid and liquid crystals, composite materials, as well as atomic vapors.

The observations and comparison of Talbot self-replications from 2-fold and 6-fold rotational symmetry masks shown in Fig. 1a,b seem very interesting. The 6-fold symmetry mask has nearly equidistant disposition of holes in radial and azimuthal direcrions. For 2-fold symmetry mask, since the period of this mask is different along the X and Y-directions, one can expect the different fractional replications from different parts of the mask at the same Talbot distance. These experiments are in progress and will be reported elsewhere.

5. Conclusion

The technique of optical induction of 2D and 3D periodic lattices in photorefractive materials based on rotational symmetry diffraction masks Talbot self-replications was studied experimentally. 1D and 2D different rotational symmery diffraction masks with the periods of few tens micrometers were prepared and 532 nm cw laser beam was used in experiments to form an intensity modulated light beam profile. The interferometric testing of prepared masks was performed showing their high quality. Talbot effect from 1D annular mask was observed: 20 high contrast self-replications of annular mask at multiples of Talbot distance Z_T, as well as the grating self imaging with half period of the original grating at $Z_T/2$ were detected. The spatial modulated intensity pattern from 1D annular mask with 100 circles and 30 μm radial period was imparted into the Fe doped lithium niobate crystal via electro-optic effect, thus creating refractive index lattice. The recorded lattice was tested by phase microscope. The spatial frequency doubling of the recorded lattice due to fractional Talbot effect was observed in the depth scanned phase microscope images. The physical mechanism of recording of photonic lattices in photorefractive LN:Fe crystal is discussed. The obtained results show the possibility of the use of 2D masks for the creation of 3D photonic lattices in photorefractive materials, which can be used as photonic crystals.

Acknowledgments

This work is supported by International Science and Technology Center Grant, Project A-1517.

References

[1] Collier, R. J., Buckhard, Ch. B., & Lin, L. H. (1971). *Optical Holography*, Academic Press, New York.

[2] Lee, Wai-Hon. (1978). In: *Progress in Optics, Editor Emil Wolf, Vol. XVI, Chapter 3, "Computer Generated Holograms: Techniques and Applications*", North-Holland, pp. 121–232.
[3] Denz, C., Schwab, M., & Weilnau, C. (2003). *Transverse-pattern Formation in Photorefractive Optics*, Springer.
[4] "Photorefractive materials, effects and devices. Control of light and matter", *Applied Physics B,* special issue, V. *95*, N.3 (2009).
[5] Chandrasekhar, S. (1977). *Liquid Crystals*, Cambridge University Press.
[6] Bortolozzo, U., Residori, S., Petrosyan, A., & Huignard, J. P. (2006). "Pattern formation and direct measurement of the spatial resolution in a photorefractive liquid-crystal-light-valve", *Opt. Commun.*, *263*, 317–321.
[7] Simoni, F., Chipparrone, G., Umeton, C., Arabia, G., & Chidichimo, G. (1990). "Nonlinear optical effects in polymer dispersed liquid crystals", *Mol. Cryst. Liq.Cryst. 179*, 269–275.
[8] Hikmet, R. A. M., & Lub, J. (1996). "Anisotropic networks and gels obtained by photo-polymerization in the liquid crystalline state: synthesis and applications", *Prog. Polym. Sci. 21*, 1165–1209.
[9] Galstian, T. V., Zohrabyan, L., Albu, A. M., Rusen, E., Marculescu, B., & Vasilescu, D. S. (2004). "Polymer stabilized liquid crystal system containing a performed polymer guest", *J. Nonlinear Optics, Quantum Optics*, *32*, 1–11.
[10] Ren, H., Fan, Y. H., & Wu, S.-T. (2003). "Prism grating using polymer stabilized nematic liquid crystals", *Appl. Phys. Lett. 82*, 3168–3170.
[11] Cheben, P., & Calvo, M. L. (2001). "A photopolymerizable glass with diffraction efficiency near 100% for holographic storage", *Appl. Phys. Lett. 78*, 1490–1492.
[12] Del Monte, F., Cheben, P., Martinez-Matos, O., Rodrigo, J. A., & Calvo, M. L. (2006). "A volume holographic sol-gel material with large enhancement of dynamic range by incorporation of high refractive index species", *Adv. Mater. 18*, 2014–2017.
[13] Martinez-Matos, O., Rodrigo, J. A., Calvo, M. L., & Del Monte, F. (2007). "Diffusion study in tailored gratings recorded in photopolymer glass with high refractive index species", *Appl. Phys. Lett. 91*, 1411151–1411153.
[14] Calvo, M. L., & Cheben, P. (2009). "Photopolymerizable sol-gel nanocomposites for holographic recording", *J. Opt. A, Pure Appl. Opt. 11*, 1–11.
[15] Ackemann, T., & Lange, W. (2001). "Optical pattern formation in alkali metal vapors: Mechanisms, phenomena and use", *Applied Physics B*, *72*, 21–34.
[16] Korneev, N., & Benavides, O. (2008). "Mechanisms of holographic recording in rubidium vapor close to resonance", *JOSA B*, *25*, 1899–1906.
[17] Yablonovitch, E. (1987). "Inhibited spontaneous emission in solid-state physics and electronics", *Phys. Rev. Lett. 58*, 2059–2062.
[18] Krauss, T. F., & De La Rue, R. M. (1999). "Photonic crystals in the optical regime – past, present and future", *Progress in Quantum Electronics*, *23*, 51–96.
[19] Joannopoulos, J., Johnson, S., Meade, R., & Winn, J. (2008) *Photonic Crystals*, Princeton Univ. Press.
[20] Cerqueira, S. Arishmar Jr. (2010). "Recent progress and novel applications of photonic crystal fibers", *Rep. Prog. Phys. 73*, 024401 (1–21)
[21] Adibi, A., Buse, K., & Psaltis, D. (2001). "Two-center holographic recording", *JOSA B*, *18*, 584–601.
[22] Fleischer, J. W., Segev, M., Efremidis, N. K., & Christodoulides, D. N. (2003). "Observation of two-dimensional discrete solitons in optically induced nonlinear photonic lattices", *Nature*, *422*, 147–150.
[23] Badalyan, A., Hovsepyan, R., Mekhitaryan, V., Mantashyan, P., & Drampyan, R. (2011). "New holographic method for formation of 2D gratings in photorefractive materials by Bessel standing wave", in *Fundamentals of Laser Assisted Micro- and Nanotechnologies 2010*, edited by Vadim P. Veiko, Tigran A. Vartanyan, Proceedings of SPIE, Vol. 7996 (SPIE Bellingham, WA, 2011) 799611–1-9.

[24] Badalyan, A., Hovsepyan, R., Mekhitaryan, V., Mantashyan, P., & Drampyan, R. (2011). "Combined interferometric-mask method for creation of micro- and sub-micrometric scale 3D structures in photorefractive materials", in *International Conference on Laser Physics 2010*, edited by Aram V. Papoyan, Proceedings of SPIE Vol. 7998 (SPIE Bellingham, WA, 2011) 7998 OH-1–10.
[25] Patorski, K.,(1989). In: Progress in Optics, E. Wolf, Editor, Vol XXVII, Chapter 1, "*The self-imaging phenomenon and its applications*", Elsevier, Amsterdam, pp. 2–108.
[26] Talbot, H. F. (1836). "Facts relating to optical science", *Phil. Mag. 9*, 401–407.
[27] Lord Rayleigh. (1881). "On copying-diffraction gratings, and some phenomena connected therewith", *Phil. Mag. 11*, 196–205.
[28] Wintrop, J. T., Worthington, C. R. (1965). "Theory of Fresnel images. I. Plane periodic objects in monochromatic light", *J. Opt. Soc. Am. 55*, 373–381.
[29] Berry, M. V., & Klein, S. (1996). "Integer, fractional and fractal Talbot effect", *J. Mod. Optics*, *43*, 2139–2164.
[30] Chapman, M. S., Ekstrom, C. R., Hammond, T. D., Schmiedmayer, J., Tannian, B. E., Wehinger, S. & Pritchard, D. E. (1995). "Near field imaging of atom diffraction gratings: the atomic Talbot effect", *Phys. Rev. A 51*, R14–R17.
[31] Deng, L., Hagley, E. W., Denschlag, J., Simsarian, J. E., Edwards, M., Clark, C. W., Helmerson, K., Rolston, S. L., & Phillips, W. D. (1999) "The temporal, matter-wave-dispersion Talbot effect", *Phys. Rev. Lett. 83*, 5407–5411.
[32] Berry, M., Marzoli, I., & Schleich, W. (2001). "Quantum carpets, carpets of light", *Physics World*, June, 39–44.
[33] Guerineau, N., Harchaoui, B., Primot, J., & Heggarty, K. (2001). "Generation of achromatic and propagation invariant spot arrays by use of continious self-imaging gratings", *Optics Letters*, *26*, 411–413.
[34] Iwanow, R., May-Arrioja, D. A., Christodoulides, D. N., Stegeman, & G. I., Min, Y. (2005). "Discrete Talbot effect in waveguide arrays", *Phys. Rev. Lett. 95*, 053902.
[35] Bortolozzo, U., Residori, S., & Huignard, J. P. (2006). "Talbot effect to enhance the two-wave-mixing gain in a stack of thin nonlinear media", *Opt. Lett. 31*, 2166–3168.
[36] Testorf, M., Suleski, Th. J., & Chuang, Yi-Chen. (2006). "Design of Talbot array illuminators for three-dimensional intensity distributions", *Optics Express*, *24*, 7623–7629.
[37] Courtial, J., Whyte, G., Bouchal, Z., & Wagner, J. (2006). "Iterative algorithm for holographic shaping of non-diffracting and self-imaging light beams", *Opt. Express*, *14*, 2108–2116.
[38] Chang, Y., Wen, J., Zu, S. N., & Xiao, M. (2010). "Nonlinear Talbot effect", *Phys. Rev. Lett.*, *104*, 183901–1-4.
[39] Adibi, A., Buse, K., & Psaltis, D. (2001). "The role of carrier mobility in holographic recording in $LiNbO_3$", *Appl. Phys. B*, *72*, 653–659.
[40] Chen, F. S.,(1969). "Optically induced change of refractive indices in $LiNbO_3$ and $LiTaO_3$", *J. Appl. Phys. 40*, 3389–3396.
[41] Glass, A. M., von der Linde, D., & Negran, T. J. (1974). "High-voltage bulk photovoltaic effect and the photorefractive process in $LiNbO_3$", *Appl. Phys. Lett. 25*, 233–235.
[42] Avanesyan, G. T., Vartanyan, E. S., Mikaelyan, R. S., Hovsepyan, R. K., & Pogosyan, A. R. (1991). "Mechanisms of photochromic and photorefractive effects in doubly doped lithium niobate crystal", *Phys. Stat. Sol. (a)*, *126*, 245–252.
[43] Günter, P., & Huignard, J. P. (2007). *Photorefractive Materials and Their Applications III, Springer Series in Optical Sciences, Vol. 115*, New York.
[44] Yang, Y., Nee, I., Buse, K., & Psaltis, D. (2001). "Ionic and electronic dark decay of holograms in $LiNbO_3$:Fe crystals". *Appl. Phys. Lett. 78*, 4076–4078.
[45] Nee, I., Muller, M., Buse, K., & Kratzig, E. (2000). "Role of iron in lithium-niobate crystals for the dark-storage times of holograms", *J. Appl. Phys. 88*, 4282–4287.
[46] Amodei, J. J., & Staebler, D. L. (1971). "Holographic pattern fixing in electro-optic crystals", *Appl. Phys. Lett. 18*, 540–542.
[47] Staebler D. L., Burke W. J., Phillips W., & Amodei J. J. (1975). "Multiple storage and erasure of fixed holograms in Fe-doped $LiNbO_3$", *Appl. Phys. Lett. 26*, 182–184.

[48] Amodei, J., Phillips, W., & Staebler, D. (1972). "Improved electrooptic materials and fixing techniques for holographic recording", *Appl. Opt. 11*, 390–396.

[49] Von der Linde, D., Glass, A. M., & Rodgers, K. F. (1974). "Multiphoton photorefractive processes for optical storage in $LiNbO_3$", *Appl. Phys. Lett. 25*, 155–157.

[50] Mantashyan, P., "Photochromic effect and holographic recording in doubly doped $LiNbO_3$ crystals" in *International Conference on Laser Physics 2010*, edited by Aram V. Papoyan, Proceedings of SPIE Vol. 7998 (SPIE Bellingham, WA, 2011) 7998 OJ-1–8.